

Evaluation of the 3D-PIV Standard Images (PIV-STD Project)

Okamoto, K.*¹, Nishio, S.*², Kobayashi, T.*³, Saga, T.*³ and Takehara, K.*⁴

*1 Nuclear Engrg. Res. Lab., The University of Tokyo, Tokai-mura, Ibaraki 319-1106, Japan.

*2 Dept. Maritime Science, Kobe University of Mercantile Marine, Kobe, Hyogo, 658-0022, Japan.

*3 Institute of Industrial Sci., The University of Tokyo, Roppongi, Tokyo, 106-8558, Japan.

*4 Dept. Civil Engineering, Kinki University, Higashi-Osaka, Osaka, 577-8502, Japan.

Received 12 January 2000.

Revised 13 April 2000.

Abstract: Particle Imaging Velocimetry (PIV) offers many advantages for studies of fluid flows. Lots of PIV techniques have been developed and applied to various flow fields. However, there are no standard tools for evaluation of the PIV system effectiveness and accuracy. To popularize the PIV for practical use, the PIV system should have some standard.

The Visualization Society of Japan (VSJ) started a project for PIV standardization and popularization in 1996 (PIV-STD Project). The PIV has two processes, i.e., the image capture with visualization and image analysis. In order to evaluate the image analysis system for the PIV, standard images were proposed. Using the images, an evaluation of the effectiveness and accuracy for the PIV system will be carried out. The developed PIV standard images are distributed using the Internet, (<http://www.vsj.or.jp/piv>). The standard images include the two-dimensional and transient three-dimensional images. The correct velocity vectors and correct particle location in three-dimensional field are also provided to evaluate the effectiveness of the target flow field.

Keywords: 3D-PIV, standard image, transient, evaluation, particle recognition.

1. Introduction

The Particle Imaging Velocimetry (PIV) is a quantitative velocity measurement technique, with visualizing the flow field by small tracer particles and with analyzing the visualized digital images. The PIV can measure the whole two-dimensional or three-dimensional flow field simultaneously without disturbing the flow field. Comparing with the traditional measurement technique, e.g., Laser Doppler Velocimeter and Hot Wire Anemometer, the whole field measurement is a great advantage to investigate the flow field.

Lots of PIV techniques have been developed and applied to various flow fields. The techniques include Cross-correlation technique (e.g., Adrian, 1991), Four-step particle tracking technique (e.g., Kobayashi et al., 1989), and so on. The developers analyzed the effectiveness of their PIV techniques using their own evaluation. There are no standard evaluation tools for investigating these PIV techniques, resulting in no standard PIV techniques. Therefore, the users should determine the selection of the appropriate PIV technique without any useful information. When the users could get the velocity distribution using some PIV technique, there also were no standard evaluation tools for the measured velocity data. In order to get the accuracy information of the measured data, they have to evaluate the data by themselves. Also, the PIV system needs lots of know-how, because the PIV system contains many steps, i.e., test section fabrication, visualization, image capture, image analysis, particle tracking, and evaluation of accuracy.

The current status of the PIV technique is far from the popularization or generalization technique. To popularize the PIV technique for practical use, the PIV standards and the PIV guide tools should be settled. With using the PIV standards, any user can easily apply the PIV technique onto their target flow field with the accuracy information.

The Visualization Society of Japan (VSJ) started a project for PIV standardization and popularization in 1996 (JPIV). The objectives of the JPIV are to popularize the complicated PIV system, and to be a standard tool for the measurement of flow field. The activities of the JPIV are summarized as follows,

- Development of Standard Images for 2D and transient 3D PIV
- Analysis using the Standard Experimental Problems
- Development of PIV Database.

The PIV technique is roughly classified into two steps, i.e., Visualization and Image Analysis. In the standard image project, the standard for the Image Processing technique for PIV is focused. The Image Processing includes image enhancement, particle detection, particle tracking, image cross correlation, velocity averaging and erroneous evaluation.

The JPIV (Okamoto et al., 1997) developed the 2D-PIV standard images with considering the three-dimensional motion. The developed PIV standard images are distributed using the Internet, (<http://www.vsj.or.jp/piv>). We provided the several Standard Images with several parameters. However, the images were based on the stable velocity distributions. Therefore they could not be applied to the evaluation of three-dimensional turbulence measurement. Therefore the PIV standard images were improved to treat the transient three-dimensional motion (Okamoto et al., 1998). The standard PIV images were based on the transient three-dimensional flow field. The flow field was illuminated by the laser light sheet or cylindrical laser light. The three-dimensional motion was shown in the images. The images were taken from several different angles. The developed PIV standard images are also distributed using the Internet (<http://www.vsj.or.jp/piv>). In the above home page of PIV standard images, the correct particle 3D locations and correct velocity distributions were also provided. Because the correct three-dimensional motions were known, the effectiveness and accuracy for the image processing technique could be easily checked. Particle 3D position extraction was one of the problems for 3D PIV. Using the standard images, the extraction algorithm could be also checked.

2. Standard Images

2.1 Target Flow Field

Using the standard images, the three-dimensional velocity field will be reconstructed by the PIV techniques. The information of the transient 3D flow field should be known, because the comparison between the reconstructed velocity field and the correct velocity field should be carried out to evaluate the effectiveness of the PIV technique. The standard images are generated by the computer graphics. The generated images should be close to the actual PIV images. Transient and three-dimensional effects should be taken into account.

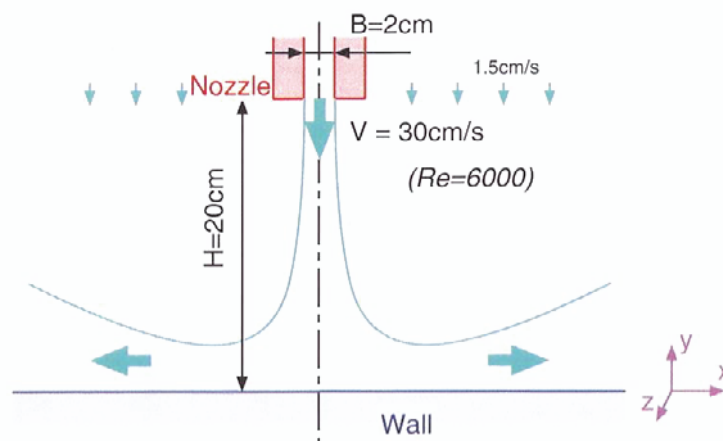


Fig. 1. Schematic of the target flow field.

The velocity vector calculated by the three-dimensional Large Eddy Simulation (LES) code is selected as the target flow field (Tsubokura et al., 1997). The flow field is the same with the previous two-dimensional standard images (Okamoto et al., 1997). Figure 1 shows the schematic view of target flow field. The two-dimensional plane jet impinges on the wall, with jet Reynolds number, 6000, i.e., turbulent. There are lots of vortices with various scales. The simulation volume is $53B \times 10B \times 3.9B$ for x, y, z -directions, where B is the nozzle width. The volume is divided into $300 \times 100 \times 34$ meshes with a variable mesh size. The flow field is solved using the LES technique. The transient three-dimensional velocity distribution in certain target volume is extracted from the simulation results with every 15 msec. The particle movement in the image is calculated using the extracted transient three-dimensional velocity vector. For the calculation of the three-dimensional velocity of the certain particle, the vector in the staggered grid system is interpolated linearly.

Figure 2 shows the example of the instantaneous in-plane ($x-y$) velocity distribution of the simulated flow field around the nozzle exit and the impinging point. The injected jet impinges on the wall resulting in higher turbulent flow, then the jet flows along the wall. The three-dimensional vortices are generated and transferred to downstream.

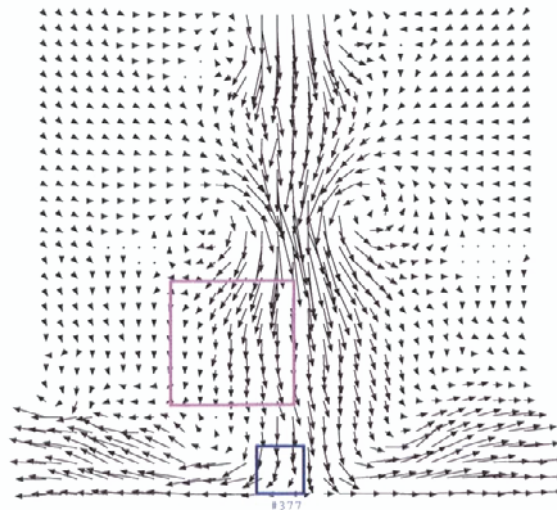


Fig. 2. Velocity distribution of the target flow field (Boxes denote the view area of the Standard Images).

2.2 Particle Image

The global coordinate system (x, y, z) is defined as shown in Fig. 1. With considering the camera location and the orientation vector, the global coordinate has been transformed to the camera coordinate system with a simple linear transformation. Then, the particle projection (X, Y) on the camera is calculated with considering the refraction at the vessel wall. Figure 3 shows the schematic of the consideration of the wall refraction under the sheet illumination. To determine the refracted light path, the light path length between the camera focus and the particle is minimized.

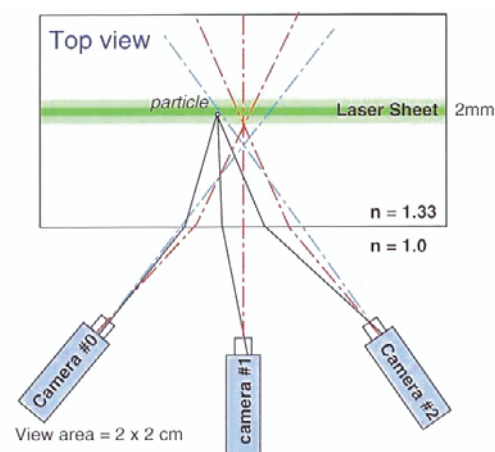


Fig. 3. Configuration for stereo PIV (No. 337).

The image size is fixed to be 256×256 pixel. One pixel has 256 intensity level (8 bit). The particle image is generated with writing the particle onto the image (Raffel et al., 1998). The intensity at the location (X, Y) in the image caused by the scatter from the particle (x_p, y_p, z_p) , whose projection is (X_p, Y_p) , is expressed as follows,

$$I(X, Y) = I_0 \exp\left(-\frac{(X - X_p)^2 + (Y - Y_p)^2}{(d_p / 2)^2}\right) \quad (1)$$

In order to emulate the laser illumination, the maximum intensity (I_0) is defined with considering the particle location. For example, under the cylindrical light illumination, it is expressed as,

$$I_0 = 240 \exp\left(-\frac{z_p^2 + x_p^2}{\sigma_l^2}\right) \quad (2)$$

where $2\sigma_l$ is the diameter of the cylindrical light.

As an initial condition, the particles are randomly generated in a certain volume. The diameter of the particle is also determined by a random generator with considering the average and standard deviation of the diameter. The diameter distribution follows the Gaussian. The particle location is shifted with considering the velocity, resulting in the new particle locations in the next image. For the integration of the particle movement, the smaller time step ($\Delta t = 0.1$ msec) is applied. Then, the new images are generated in every 2 to 5 msec, with using Eqs. (1) and (2). This procedure is repeated for certain repetition time.

2.3 Three-dimensional Standard Image

The PIV standard images are distributed with using the Internet. The URL of the images is <http://www.vsj.or.jp/piv>. Anybody can download the standard image file through anonymous FTP or HTML. Also, the free CD-R is delivered who needs a huge data transforms.

Table 1 shows the characteristics of the transient three-dimensional PIV Standard images. There are four categories of the images.

Table 1. Summary of 3D-PIV standard images.

No.	N	n	T	Comments
301	3000	1.00	720	2C2D
302	500	1.00	720	2C2D
331	4000	1.33	720	3C2D
337	4000	1.33	400	3C2D
351	2000	1.33	720	3C3D
352	300	1.33	720	3C3D
375	500	1.33	720	3C3D
377	500	1.33	200	3C3D

N : Number of Particles n : Refraction index of the water and wall T : Time series (ms)

- Transient Two-dimensional Image

(2 Components in 2 Dimension)

In Nos. 301 and 302, the flow field is illuminated by the two-dimensional laser light sheet. The two-dimensional cross-section is visualized so that the two-components of the velocity vectors could be measured. The displacement of the particle is 0 to 10 pixels/interval. Three-dimensional motion (out-of-plane) is about 10% of the laser light sheet thickness.

- Stereo PIV Image

(3 Components in 2 Dimension)

To check the stereo PIV system, the Nos. 331 and 337 are provided. The flow field is also visualized using the two-dimensional laser light sheet as shown in Fig. 3. The visualized field is captured by the three-cameras, which are set horizontally. Since the laser light sheet has 2 mm thickness, the particle three-dimensional motions are recorded on the image. The out-of-plane motion is about 10 to 20% of the laser thickness. Also, complicated vortex motions are simulated, resulting in the 3 components to be captured.

Three cameras are settled on a horizontal plane. Center camera (#1) is located on the z axis, i.e., perpendicular to x - y plane. The vessel wall is also settled on a parallel to the x - y plane. So, camera #1 has small refraction effects. While, left and right cameras (#0, #2) are set with the angle of 30 degree to z axis. Because of the refraction, the particle images are distorted. The refraction index in the water and wall is 1.33.

- Simple 3D-PIV Image

(3 Components in 3 Dimension)

A cylindrical laser light volume illumination is used for Nos. 351 and 352. The both series contain 145 serial images (720 ms) with transient three-dimensional flow field. The flow field is the same with that of No. 301. The images with grid point particles are provided to calculate the camera position correctly. Also, the accurate particle three-dimensional position and projection point on the images are also provided as a text file. In order to calculate the particle three-dimensional positions, reconstruction procedure from the three camera images is needed. This standard images could be also applied to calibrate the three-dimensional reconstruction algorithm.

- Complex 3D-PIV Image

(3 Components in 3 Dimension)

Nos. 371 and 377 are illuminated by cylindrical laser light. In No. 371, the camera locations are almost the same with No. 351, however, they have disturbances. This disturbances simulate the uncertainty of the camera setup. The camera has inclined horizontally and vertically. In No. 377, the flow field near the wall impingement is viewed from bottom. The three cameras are settled on the corner of triangle as shown in Fig. 4. The refraction index in the water and wall is 1.33. Because the flow field at the impingement is highly turbulent, interesting particle motions are visualized.

In the current status, the evaluation of the reconstructed velocity from the PIV standard images should be done by the users with comparing the reconstructed data with the correct one. The development of standard evaluation tool will also be an important topic.

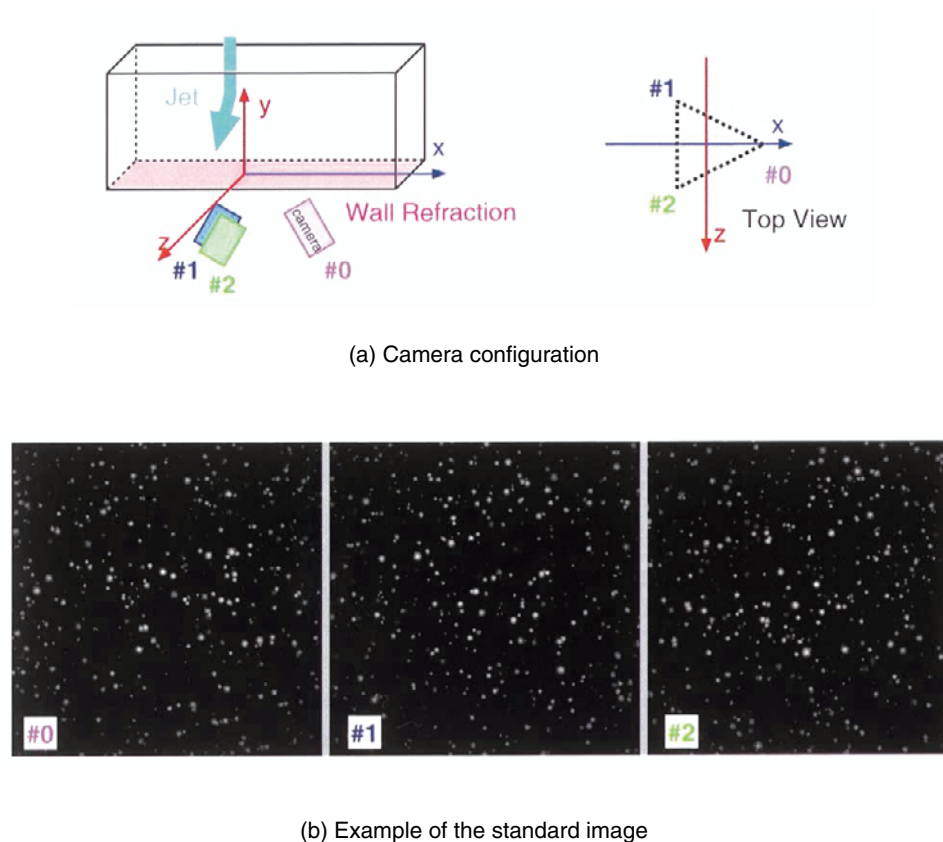


Fig. 4. Standard Image No. 377 (Complex 3D-PIV image).

3. Application of Standard Images

3.1 Particle Identification

The 2C2D and 3C2D-PIV, i.e., stereo PIV, need not identify each particles. However, in the 3C3D-PIV, every particle should be identified. Therefore, the effectiveness of the particle identification should be also taken into account. The particle centroid should be correctly identified from the particle image.

Also even in the two-dimensional PIV measurement, the Particle Tracking Technique, such as, Spring Model technique, Velocity gradient tensor technique, and so on, need the particle centroid. The accuracy of the particle centroid extraction is highly related to the accuracy of the measured vectors.

There are several techniques to capture the particle centroid from the particle images. The simplest way is the binarization using certain threshold. The problem of the binarization is the spatial resolution of the particle centroid limited to the pixel accuracy. To archive the sub-pixel accuracy, several techniques are proposed, including the particle mask technique. The images are scanned with the Gaussian mask pattern, which represents the particle intensity. The higher correlation position may be the particle centroid. Therefore, with interpolating the correlation peak with Gaussian, the sub-pixel particle centroid can be picked up.

Figure 5 shows the example of the particle image of 64×64 pixel. The center particle centroid is the $(33.21, 22.11)$. While the reconstructed centroid by these two techniques is $(33.33, 22.33)$ for binarization and $(33.22, 22.15)$ for mask technique, respectively. The accuracy of the binarization technique depends on the particle image area. Figure 6 shows the variation of the detected particle centroid from the correct centroid. They are distributed around $(0,0)$ with Gaussian distribution. The analysis of about 1000 particle data in the No. 337 image shows that the averaged error is about 0.37 pixel and 0.18 pixel, respectively.

In this example, since the particle image has no noise, the measured particle centroid has relatively good accuracy. As the number of particles increases, the occlusion of the particle occurs. Lots of particle images may be overlapped, resulting in the accuracy of the particle centroid detection to decrease.

In the actual image, the sub-pixel accuracy for the particle identification decreases because of the image

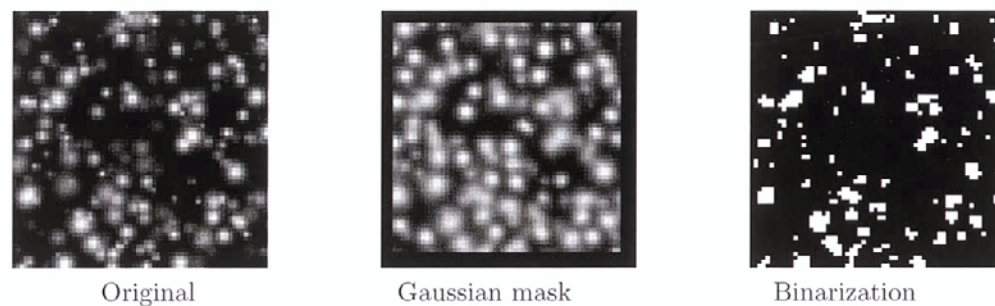


Fig. 5. Example of particle image.

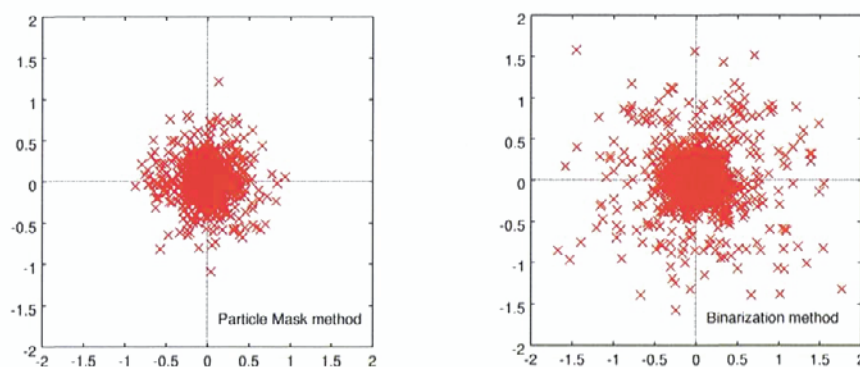


Fig. 6. Particle centroid error.

noises. However, the accuracy of the measured velocity highly depends on the particle centroid. To detect high accurate centroid, the particle image diameter should be large enough to get the high accurate centroid. Also, the number of the particles should be small enough to avoid the overlapping.

3.2 Three-dimensional Tracking

Using the provided three-dimensional Standard Image, No. 377, the evaluation of a three-dimensional particle tracking algorithm was demonstrated.

3.2.1 Parameters

In this study, the evaluation parameters were taken as the average displacement (\bar{d}_m). The flow field is about $0.5\text{cm} \times 0.5\text{cm} \times 0.5\text{cm}$ in cubic (V). Particles were distributed almost uniform inside the cubic area. The particle displacement was the function of the location. Average displacement was determined as the averaged displacement of all particle during the image interval. By varying the time interval between the two images, the average displacement (\bar{d}_m) was varied. To normalize the average displacement, the average particle distance was taken as the normalized length. The average particle distance is expressed as,

$$d_{av} = (6V/\pi N)^{\frac{1}{3}}, \quad (3)$$

where N denotes the number of particles in the target field (V). So, normalized displacement ($\delta = \bar{d}_m/d_{av}$) is defined as the ratio between displacement and average distance.

In the No. 377 images, about 1000 particles were visible from three cameras. While, the particles recorded onto all of the three-cameras were only 500. Because the illumination was volumetric, the particles outside the target flow fields were also visible. Therefore, only 100 particles existed inside the target field, ($5\text{mm} \times 5\text{mm} \times 5\text{mm}$).

In the Spring Model, the number of particles in one particle cluster was fixed to be n_{cluster} .

3.2.2 Evaluation

Because the flow field was transient, the correct flow field was varied with time. The standard image contained the 200 msec data with every 1 msec. In this study, the time interval between the two images was selected as the average displacement parameter.

Figures 7 and 8 show the reference and the reconstructed velocity distributions of the target field, respectively. The velocity field was visualized in the span-wise direction. The view direction was almost the $-x$ direction, therefore, the y - z velocity was mainly visualized. In the figure, the miss-track vector was displayed as the red line. The large vortex field was reconstructed correctly. With increased time interval, i.e., the average displacement, the tracking efficiency decreased.

Even in the larger particle displacement, the particles in the central region were tracked correctly. However, because of the flow out particles, the edge area of the flow field could not be tracked.

As the evaluation parameter, the ratio of the correct particles to all particles to be tracked was taken. The all particles included the miss-track particles, but excluded the particles which flowed out the field during the time

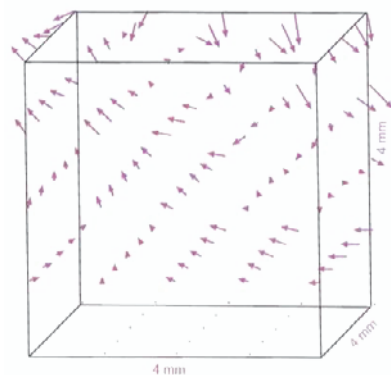


Fig. 7. Reference three-dimensional flow field ($t = 100$).

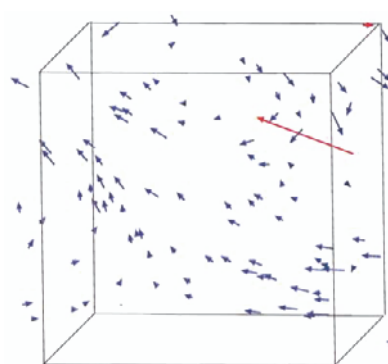


Fig. 8. Reconstructed three-dimensional velocity distributions ($\Delta t = 10 \text{ msec}/d_m/d_a = 0.5$).

interval. It expresses the effectiveness of the particle tracking.

Figure 9 shows the relationship between the ratio and the average displacement. By increasing the average displacement, the correct tracking ratio decreased rapidly. When the displacement of the particle (\bar{d}_m) exceeded the half of the particle distance (d_{av}), number of the miss-track particle increased. Because the miss-track particle existed in the edge of the target region, the velocities could be correctly tracked inside the field even when the displacement was large.

The number of particles in one cluster ($n_{cluster}$) was varied from 18 (standard case for Spring Model) to 12 or 6. With decreased number of particles on one cluster, the interrogation region also decreased. Therefore, the miss-track occurred even in the small displacement. However, under the larger displacement case, the ratio for correct vectors were almost the same with the standard case ($n_{cluster} = 18$). By decreasing the particle numbers in one cluster, the calculation time decreased. In this study, the number of particles in the flow field was only 100. So, the number of particle in one cluster did not affect the tracking efficiency. In the actual cases, the smaller $n_{cluster}$ led the miss-tracking, while it also led the fast calculation.

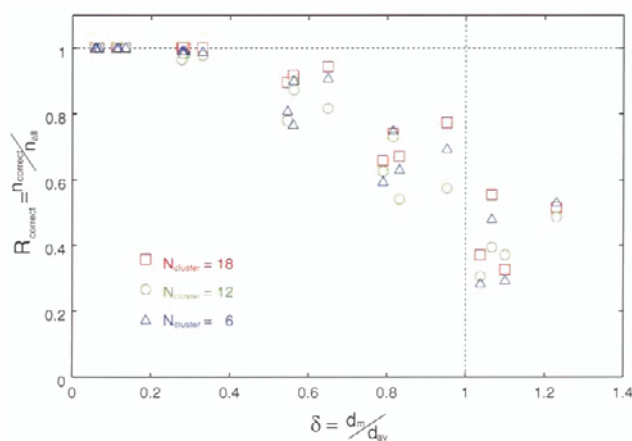


Fig. 9. Relationship between tracking efficiency and displacement.

4. Conclusions

The standard images which aim to establish an evaluation code of PIV were proposed. The standard images have been developed based on the calculated velocity field by means of three-dimensional LES. The transient and three-dimensional motions are taken into account in the standard images. To generate the images, the wall refraction at the vessel surface is considered. The effectiveness of the present standard images is demonstrated using the Spring model technique.

References

- Adrian, R. J., Particle-imaging techniques for experimental fluid mechanics, *Ann. Rev. Fluid Mech.*, Vol. 23, (1991) 261.
- Gharib, M., Center for Quantitative Visualization, <http://www.cqv.caltech.edu/> (1995).
- Kobayashi, T., Saga T., Segawa, S. and Knada, H., Development of a Real-Time Velocity Measurement System for Two-Dimensional Flow Fields Using a Digital Image Processing Technique, *Trans. of JSME (B)*, Vol. 55, No. 509, (1989) 107.
- Okamoto, K., Hassan, Y. A. and Schmidl, W. D., New Tracking Algorithm for Particle Image Velocimetry, *Experiment in Fluids*, Vol. 19, No. 5, (1995), 342.
- Okamoto, K., Nishio, S., Kobayashi, T. and Saga, T., Standard Images for Particle Imaging Velocimetry, *Proc. PIV'97-Fukui*, Fukui, 229 (1997).
- Okamoto, K., Kobayashi, T., Saga T. and Nishio, S., Particle imaging velocimetry standard images for transient three-dimensional flow, *Proc. 9th Int. Symp. Application of Laser Tech. to Fluid Mech.*, Lisbon, 13.4.1 (1998).
- Raffel, M., Willert, C. and Kompenhans, J., *Particle imaging velocimetry—a practical guide*, Springer-Verlag, Berlin (1998).
- Tsubokura, M., Kobayashi, T. and Taniguchi, N., Visualization of 3-D structures in a plane impinging jet using Large Eddy Simulation, *Proc. FLCOME'97*, Vol. 2, 875 (1997).

Author Profile

Koji Okamoto: He received his MSc (Eng) in Nuclear Engineering in 1985 from University of Tokyo. He also received his Ph.D in Nuclear Engineering in 1992 from University of Tokyo. He worked in Department of Nuclear Engineering, Texas A&M University as a visiting associate professor in 1994. He works in Nuclear Engineering Research Laboratory, University of Tokyo as an associate professor since 1993. His research interests are Quantitative Visualization, PIV, Holographic PIV, Flow Induced Vibration and Thermal-hydraulics in Nuclear Power Plant.



Shigeru Nishio: He graduated from Osaka University in 1983 and received his M.Eng. degree in Naval Architecture in 1985. He worked in Department of Marine System Engineering, Osaka Prefecture University from 1988 to 1999. He was awarded Ph. D. (Eng) degree in ship hydrodynamics, study on the three-dimensional separated flow around prolate spheroids and ships at incidence in 1990. He has been working as an Associate Professor in Kobe University of Mercantile Marine, Department of Maritime Science since 1999. His research interests are in the image measurement of flow field and the bio-fluid mechanics in fish-like propulsions.



Toshio Kobayashi: He received his Ph. D. in Mechanical Engineering Department, the University of Tokyo in 1970. After completion of his Ph. D. program, he has been a faculty member of Institute of Industrial Science, University of Tokyo, and currently is a Professor. His research interests are numerical analysis of turbulence, especially Large Eddy Simulation (LES), and particle imaging velocimetry (PIV) technique. He serves as the President to the Visualization Society of Japan (VSJ), President-elect to the Japan Society of Mechanical Engineers (JSME), and Executive Vice President to the Society of Automotive Engineer of Japan (JSAE).



Tetsuo Saga: He works in the Institute of Industrial Science, University of Tokyo. His research field is mechanical engineering. Flow visualization and its image analysis, prediction and control of flow induced vibration, automobile aerodynamics are his main research works. His current research interests are in micro- and bio-flow analysis by using PIV.



Kohsei Takehara: He received his BSc (Eng.) degree in Civil Engineering in 1986 from Kyushu Institute of Technology, his MS degree in 1988 and Ph.D. in 1997 from Kyushu University. After he received his MS degree, he worked as a research associate at Kinki University. He took his current position as assistant professor at Kinki University in 1996. He worked in Department of Theoretical and Applied Mechanics, University of Illinois at Urbana-Champaign as a visiting scholar in 1998. His research interests include the gas transfer at water surface, the development of PTV technique, etc.